matching. This is because the eigenreflection coefficients of both devices are separated by 90° on the unit circle. Furthermore, it was shown that this condition is identically satisfied for all frequencies for a 2-branch coupler, provided that the ratio of the in-line to branch-line admittance levels is $\sqrt{2}$. This fact was used to construct a compact stripline hybrid operating at 400 MHz using lines which are a quarter wavelength long at 1 GHz.

VII. Appendix

It is obvious that the results in the text can readily be generalized to the case of the n-port circulator where the n eigenvalue phase angles must be separated by $360/n$ degrees on the unit circle for perfect circulation. Here the results will only be stated for the five-port circulator at the reference plane where $\psi_0 = 180°$. The eigenadmittances at such a plane are $jY_0^* = j\infty$, jY_{-1}^*, jY_1^*, jY_{-2}^*, and jY_2^*. The real and imaginary parts of the equivalent admittance are

$$G^* = \frac{Y_1^* - Y_{-1}^*}{2} \cdot \tan 36° = \frac{Y_2^* - Y_{-2}^*}{2} \cdot \tan 72°$$

$$Y^* = \frac{Y_1^* + Y_{-1}^*}{2} = \frac{Y_2^* + Y_{-2}^*}{2}.$$

It is apparent that two conditions on the eigenadmittances must be satisfied before a circulator can be obtained by matching alone. In the general n-port case, $n-3$ conditions must be satisfied.

References

[1] J. W. Simon, "Broadband strip-transmission line y-junction circulators," *IEEE Trans. Microwave Theory Tech.*, vol. MTT-13, pp. 335–345, May 1965.

[2] E. Pivit, "Zirkulatoren aus Konzentrierten Schaltelementen," *Telefunken J.*, vol. 38, p. 206, 1965.

[3] J. Deutsch and B. Wieser, "Resonance isolator and y-circulator with lumped elements at VHF," *IEEE Trans. Magn.*, vol. MAG-2, pp. 278–282, Sept. 1966.

[4] R. H. Knerr, "A proposed lumped-element switching circulator principle," *IEEE Trans. Microwave Theory Tech.*, vol. MTT-20, pp. 396–401, June 1972.

[5] G. P. Riblet, "The notion of an equivalent admittance for symmetrical non-reciprocal 3 port networks," presented at *Proc. 1976 IEEE Int. Symp. Circuits and Systems*, Apr. 1976.

[6] ——, "The measurement of the equivalent admittance of 3 port circulators via an automated measurement system," *IEEE Trans. Microwave Theory Tech.*, vol. MTT-25, pp. 401–405, May 1977.

[7] J. Helszajn, *Nonreciprocal Microwave Junctions and Circulators*. New York: Wiley, 1975.

[8] J. B. Davies and P. Cohen, "Theoretical design of symmetrical junction stripline circulators," *IEEE Trans. Microwave Theory Tech.*, vol MTT-11, pp. 506–512, Nov. 1963.

[9] C. G. Montgomery, R. H. Dicke, and E. M. Purcell, *Principles of Microwave Circuits*. New York: McGraw-Hill, 1948.

[10] G. P. Riblet, "A directional coupler with very flat coupling," *IEEE Trans. Microwave Theory Tech.*, vol. MTT-26, Feb. 1978.

Field Theory Treatment of *H*-Plane Waveguide Junction with Triangular Ferrite Post

ABDEL-MESSIAS KHILLA AND INGO WOLFF

Abstract—**This paper presents an exact field theory treatment for the *H*-plane waveguide junction with three-sided ferrite prism. The treatment is general, being independent of the geometrical symmetry of the junction, the number of ports, and the location of the ferrite post inside the junction. The solution of the wave equations in the ferrite post and in the surrounding region is written in the form of an infinite summation of cylindrical modes. The fields at the ferrite-air interface are matched using the point-matching technique. This results in two amplitudes for the cylindrical modes describing the fields in the air region in the form of a matrix.**

The fields at the arbitrary boundary between the air region and the waveguides are also matched using the point-matching technique. This results in a finite system of nonhomogeneous equations in the field amplitudes.

The three-port waveguide junction circulator with central triangular ferrite post is analyzed using this technique.

Two specific arrangements are considered. In the first arrangement, the points of the triangles are in the centers of the waveguides, and in the second, the sides of the triangles are in the centers of the waveguides. The method used in this paper can also be applied to study the effect of the ferrite-post geometry on the circulator performance in order to seek the best possible circulator structure.

Excellent agreement has been found between published experimental measurements and the numerical results obtained by this technique in the case of a waveguide junction circulator with cylindrical ferrite post.

Manuscript received June 8, 1977; revised October 11, 1977.

The authors are with the Department of Electrical Engineering, University of Duisburg, Duisburg, Germany.

I. Introduction

THE VERSATILITY of the most widely used ferrite junction circulator is indicated by the fact that in addition to its use as a circulator, it can also be used as an isolator or as a switch. It can be constructed in either a rectangular waveguide or stripline technique. The waveguide version usually uses a *H*-plane junction.

The problem of the waveguide circulator design has been overcome by numerical techniques for some simpler structures such as latching circulators, simple ferrite-rod Y and T junctions, and various inhomogeneous ferrite cylinders (ferrite post [8]), ferrite tube–dielectric rod–dielectric sleeve, and ferrite post–metal pin–dielectric sleeve [1]–[3]).

0018-9480/78/0400-0279$00.75

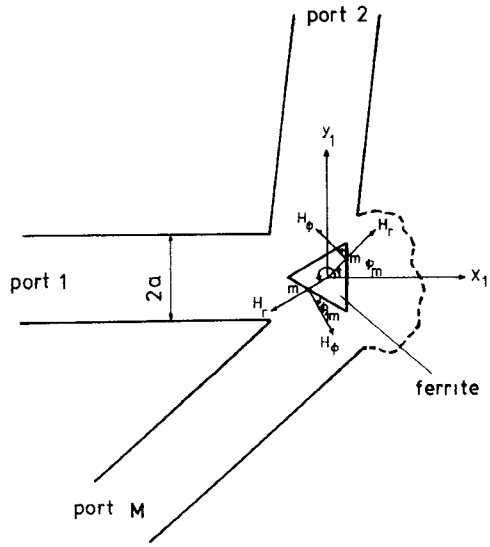

Fig. 1. Schematic representation of M-port nonsymmetrical waveguide junction with a triangular ferrite post.

Resonant modes of partial-height ferrite junction circulators were studied recently [4]–[6]. The resonance modes of a demagnetized triangular ferrite post which correspond to the eigenexcitation were classified [7], under the assumption of a completely open-circuited condition at the sidewalls of the ferrite post, which is not the case in the waveguide circulators.

The method of analysis adopted in this paper is to match the cylinderical modes in the triangular ferrite post to the cylindrical modes outside the post, which in turn are matched to the complete set of modes of the rectangular waveguides. An infinite set of equations results, each involving an infinite number of unknowns (the amplitudes of rectangular waveguide and cylindrical modes). An infinite number of equations is required to obtain an exact solution. In this problem, as in most problems solved by model methods, a closed form exact solution is not possible. However, results to a reasonable degree of accuracy can be obtained by taking into account a sufficient number of cylindrical modes at the ferrite–air interface, as well as waveguide modes and cylindrical modes at the common boundaries between the junction and the waveguide.

The junction consists of M rectangular waveguides (waveguide width 2(a)) intersecting as shown schematically in Fig. 2. These identical waveguides are assumed to propagate only the dominant TE_{10} mode, while all higher modes are cut off. A full-height rectangular ferrite post is placed inside the junction and the dc magnetic field is applied normal to the plane of the junction. The system is assumed to be free of any losses, and the electromagnetic field components have a time dependence in the form of an exponential function: $\exp(j\omega t)$. It is further assumed that the output ports are perfectly matched.

This technique is applied to the H-plane Y junction with a triangular equilateral ferrite post. Two specific cases are considered. In the first case, the points of the triangles are in the centers of the waveguides, whereas in the second case the sides of the triangles are in the centers of the waveguides.

II. Field Analysis

All fields are assumed to be independent of the z coordinate, and they are taken to have a time dependence $\exp(j\omega t)$. Rectangular and circular cylindrical coordinate systems (x,y,z) and (r,Φ,z) are employed (as shown in Fig. 1).

A complete expansion for fields in the ferrite ($r \leqslant r_m(\Phi)$), therefore [8], is

$$E_z(r,\Phi) = \sum_{n=-\infty}^{\infty} a_n J_n(k_f r)\exp(-jn\Phi) \tag{1}$$

$$H_\Phi(r,\Phi) = -jY_f \sum_{n=-\infty}^{\infty} a_n \left[J_n'(k_f r) + \frac{k}{\mu}\frac{n}{k_f r} J_n(k_f r)\right]\exp(-jn\Phi) \tag{2}$$

$$H_r(r,\Phi) = Y_f \sum_{n=-\infty}^{\infty} a_n \left[\frac{k}{\mu} J_n'(k_f r) + \frac{n}{k_f r} J_n(k_f r)\right]\exp(-jn\Phi) \tag{3}$$

$$E_r(r,\Phi) = E_\Phi(r,\Phi) = H_z(r,\Phi) = 0 \tag{4}$$

where

$$k_f = \omega\sqrt{\mu_0\epsilon_0\epsilon_r\mu_{\text{eff}}}$$

and

$$\mu_{\text{eff}} = \frac{\mu^2 - k^2}{\mu},$$

μ, k diagonal and off-diagonal permeability tensor elements in the $(x$–$y)$ plane

$$Y_f = \sqrt{\epsilon_0\epsilon_r/\mu_0\mu_{\text{eff}}}$$

ϵ_r is the relative permittivity of the ferrite material, and the coefficients a_n are the unknown field amplitudes.

Similarly, the fields outside the ferrite post ($r \geqslant r_m(\Phi)$) are of the form

$$E_z(r,\Phi)=\sum_{n=-\infty}^{\infty}\left[b_nJ_n(k_ar)+c_nY_n(k_ar)\right]\cdot\exp(-jn\Phi) \quad (5)$$

$$H_\Phi(r,\Phi)=-jY_a\sum_{n=-\infty}^{\infty}\left[b_nJ_n'(k_ar)+c_nY_n'(k_ar)\right]\cdot\exp(-jn\Phi) \quad (6)$$

$$H_r(r,\Phi)=\frac{Y_a}{k_ar}\sum_{n=-\infty}^{\infty}n\left[b_nJ_n(k_ar)+c_nY_n(k_ar)\right]\cdot\exp(-jn\Phi) \quad (7)$$

$$E_r(r,\Phi)=E_\Phi(r,\Phi)=H_z(r,\Phi)=0 \quad (8)$$

where

$$k_a=\omega\sqrt{\epsilon_0\mu_0}$$

$$Y_a=\sqrt{\epsilon_0/\mu_0}$$

b_n and c_n are the field amplitudes.

The continuity condition for $E_z(r,\Phi)$ and $H_{\tan}(r,\Phi)$ can be applied at any point $r=r_m$ along the ferrite–air interface to give

$$\sum_{n=-\infty}^{\infty}a_nJ_n(k_fr_m)\exp(-jn\Phi_m)=\sum_{n=-\infty}^{\infty}b_nJ_n(k_ar_m)\exp(-jn\Phi_m)+\sum_{n=-\infty}^{\infty}c_nY_n(k_ar_m)\exp(-jn\Phi_m) \quad (9)$$

$$\sum_{n=-\infty}^{\infty}a_nY_f\cdot\left[J_n'(k_fr_m)\left\{\frac{k}{\mu}\sin(\Phi_{1m})-j\cos(\Phi_{1m})\right\}+\frac{n}{k_fr_m}J_n(k_fr_m)\left\{\sin(\Phi_{1m})-j\frac{k}{\mu}\cos(\Phi_{1m})\right\}\right]\cdot\exp(-jn\Phi_m)$$
$$=\sum_{n=-\infty}^{\infty}b_nY_a\left\{\frac{n}{k_ar_m}J_n(k_ar_m)\cdot\sin(\Phi_{1m})-jJ_n'(k_ar_m)\cdot\cos(\Phi_{1m})\right\}\exp(-jn\Phi_m)+\sum_{n=-\infty}^{\infty}c_nYa\left\{\frac{n}{k_ar_m}Y_n(k_ar_m)\cdot\sin(\Phi_{1m})-jY_n'(k_ar_m)\cdot\cos(\Phi_{1m})\right\}\exp(-jn\Phi_m). \quad (10)$$

Φ_{1m} is the angle between the side of the ferrite triangle and $H_\Phi(r_m,\Phi_m)$, Φ_{1m} is positive when it takes the same direction as Φ_m, and negative otherwise.

Since the number of unknowns involved in these equations is infinite, an infinite number of matching points are required for an exact solution. In this case, a closed-form exact solution is not possible. However, results to a reasonable degree of accuracy can be obtained by taking a sufficient number of cylindrical modes into account.

Consider n_f cylindrical modes and q_f matching points at each side of the triangular ferrite post such that

$$2n_f+1=3q_f. \quad (11)$$

Equations (9) and (10) can then be written in the form of quadratic matrices

$$A\cdot a=B\cdot b+C\cdot c \quad (12)$$

$$A1\cdot a=B1\cdot b+C1\cdot c \quad (13)$$

where

$$A=[A_{li}],\qquad A_{li}=J_i(k_fr_l)\exp(-ji\Phi_l)$$
$$B=[B_{li}],\qquad B_{li}=J_i(k_ar_l)\exp(-ji\Phi_l)$$
$$C=[C_{li}],\qquad C_{li}=Y_i(k_ar_l)\exp(-ji\Phi_l)$$
$$A1=[A1_{li}],$$
$$A1_{li}=Y_f\cdot\left[J_i'(k_fr_l)\cdot\left\{\frac{k}{\mu}\sin(\Phi_{1l})-j\cos(\Phi_{1l})\right\}+\frac{i}{k_fr_l}J_i(k_fr_l)\cdot\left\{\sin(\Phi_{1l})-j\frac{k}{\mu}\cos(\Phi_{1l})\right\}\right]\cdot\exp(-ji\Phi_l)$$
$$B1=[B1_{li}],$$
$$B1_{li}=Y_a\cdot\left[\frac{i}{k_ar_l}J_i(k_ar_l)\sin(\Phi_{1l})-J_i'(k_ar_l)\cos(\Phi_{1l})\right]\cdot\exp(-ji\Phi_l)$$
$$C1=[C1_{li}],$$
$$C1_{li}=Y_a\cdot\left[\frac{i}{k_ar_l}Y_i(k_ar_l)\sin(\Phi_{1l})-Y_i'(k_ar_l)\cos(\Phi_{1l})\right]\cdot\exp(-ji\Phi_l)$$
$$a=[a_i],\qquad b=[b_i],\qquad c=[c_i]$$

with

$$i=-n_f,-n_f+1,-n_f+2,\cdots,n_f,$$

and

$$l=1,2,3,\cdots,3q_f.$$

Equations (12) and (13) can be combined as

$$c=Z\cdot b \quad (14)$$

where the matrix Z is given by

$$Z=(A^{-1}C-A1^{-1}C1)^{-1}\cdot(A1^{-1}B1-A^{-1}B). \quad (15)$$

The incident electromagnetic field components at port 1 are given by

$$E_z(x_1,y_1)=\sin\{(1+y_1/a)\pi/2\}\cdot\exp(-jk_1x_1) \quad (16)$$

$$H_y(x_1,y_1)=-\frac{k_1}{\omega\mu_0}\sin\{(1+y_1/a)\pi/2\}\cdot\exp(-jk_1x_1) \quad (17)$$

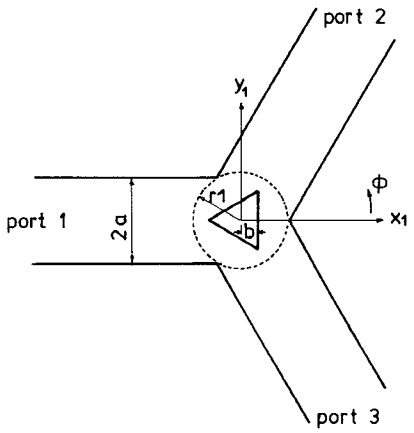

Fig. 2. Schematic representation of the Y junction with a triangular ferrite post.

$$H_x(x_1,y_1)=\frac{j}{2\omega\mu_0 a}\cos\{(1+y_1/a)\pi/2\}\cdot\exp(-jk_1x_1) \tag{18}$$

where

$$k_1=\sqrt{k_a^2-(\pi/2a)}\,.$$

A complete expansion for the scattered field in the ith waveguide can be written as

$$E_z^i(x_i,y_i)=\sum_{m=1}^{\infty} d_m^i\sin\{(1+y_i/a)m\pi/2\}\cdot\exp(jk_mx_i) \tag{19}$$

$$H_y^i(x_i,y_i)=\frac{1}{\omega\mu_0}\sum_{m=1}^{\infty} d_m^i k_m\sin\{(1+y_{i/a})m\pi/2\}\cdot\exp(jk_mx_i) \tag{20}$$

$$H_x^i(x_i,y_i)=\frac{j}{2\omega\mu_0 a}\sum_{m=1}^{\infty} d_m^i m\cos\{(1+y_i/a)m\pi/2\}\cdot\exp(jk_mx_i) \tag{21}$$

where

$$k_m=-j\sqrt{(m\pi/2a)^2-k_a^2}\,.$$

d_1^i is the complex transmission coefficient from port 1 to the ith port, $d_2^i, d_3^i, \cdots$ are the complex amplitudes of the evanescent modes in the ith waveguide, and x_i,y_i are rectangular coordinates at port i.

The matching of the fields given by (5)–(7) with the waveguide fields given by (16)–(21) along the "walls" between the air region and the waveguides depends on the geometry of the junction. As an example, a Y junction is treated.

A cylindrical wall whose axis coincides with the junction axis is chosen to be the "wall" between the air surrounding the ferrite post and the waveguides (Fig. 2).

The boundary conditions on this cylindrical wall of radius ($r1=2a/\sqrt{3}$) are, for the ith waveguide

$$E_z(r1,\Phi^i)|_{\text{air}}=E_z(x_i,y_i)|_{\text{waveguide }i} \tag{22}$$

$$H_\Phi(r1,\Phi^i)|_{\text{air}}=-H_x(x_i,y_i)\cdot\sin\Phi_i+H_y(x_i,y_i)\cdot\cos\Phi_i|_{\text{waveguide }i} \tag{23}$$

where

$$x_i=2a\cos\Phi_i/\sqrt{3}$$

$$y_i=2a\sin\Phi_i/\sqrt{3}$$

$$\Phi^i=\Phi_i+(1+i)\cdot 2\pi/3,\qquad 2\pi/3\leqslant\Phi_i\leqslant 4\pi/3.$$

Using the previous field expressions (5)–(7) and (16)–(21) with (22) and (23) gives

$$\begin{aligned}&\sum_{m=1}^{\infty} d_m^i\sin\{(1+y_i/a)m\pi/2\}\exp(jk_mx_i)\\&\quad-\sum_{n=-\infty}^{\infty} b_nJ_n\left(2ak_a/\sqrt{3}\right)\exp(-jn\Phi^i)\\&\quad-\sum_{n=-\infty}^{\infty} c_nY_n\left(2ak_a/\sqrt{3}\right)\exp(-jn\Phi^i)\\&=-\delta_{1i}\sin\{(1+y_i/a)\pi/2\}\exp(-jk_1x_i)\end{aligned} \tag{24}$$

$$\begin{aligned}&1/\omega\mu_0\cdot\sum_{m=1}^{\infty} d_m^i\left[k_m\sin\{(1+y_i/a)m\pi/2\}\cos\Phi_i\right.\\&\quad\left.-j\pi m/2a\cdot\cos\{(1+y_i/a)m\pi/2\}\sin\Phi_i\right]\\&\quad\cdot\exp(-jk_mx_i)+jY_a\sum_{n=-\infty}^{\infty} b_nJ_n'\left(2ak_a/\sqrt{3}\right)\\&\quad\cdot\exp(-jn\Phi^i)+jY_a\sum_{n=-\infty}^{\infty} c_nY_n'\left(2ak_a/\sqrt{3}\right)\\&\quad\cdot\exp(-jn\Phi^i)\\&=\delta_{1i}\cdot 1/\omega\mu_0\cdot\left[k_1\sin\{(1+y_i/a)\pi/2\}\cos\Phi_i\right.\\&\quad\left.+j\pi/2a\cdot\cos\{(1+y_i/a)\pi/2\}\sin\Phi_i\right]\\&\quad\cdot\exp(-jk_1x_i)\end{aligned} \tag{25}$$

where δ_{1i} is the Kronecker delta and $i=1$, 2, and 3 (3-port). An infinite number of equations are required to obtain an exact solution. However, results to a reasonable degree of accuracy can be obtained by taking a sufficient number of waveguide and cylindrical modes into account.

Consider m_w waveguide modes, n_a cylindrical modes, and q_w matching points in each waveguide such that

$$2n_a+1=3q_w=3m_w. \tag{26}$$

Equations (24) and (25) can be written in the form of quadratic matrices:

$$D\cdot d+E\cdot b+F\cdot c=P \tag{27}$$

$$D1\cdot d+E1\cdot b+F1\cdot c=P1 \tag{28}$$

where

$$D=\begin{bmatrix}D_{kl} & 0 & 0\\ 0 & D_{kl} & 0\\ 0 & 0 & D_{kl}\end{bmatrix};$$

$$D_{kl}=\sin\{(1+y_{1k}/a)l\pi/2\}\exp(jk_l x_{1k}),$$

$$E=\begin{bmatrix}E_{kn}^1\\ \hline E_{kn}^2\\ \hline E_{kn}^3\end{bmatrix};$$

$$E_{kn}^i=-J_n(2ak_a/\sqrt{3})\exp(-jn\Phi_k^i),$$

$$F=\begin{bmatrix}F_{kn}^1\\ \hline F_{kn}^2\\ \hline F_{kn}^3\end{bmatrix};$$

$$F_{kn}^i=-Y_n(2ak_a/\sqrt{3})\exp(-jn\Phi_k^i),$$

$$D1=\left[\begin{array}{c|c|c}D1_{kl}&0&0\\ \hline 0&D1_{kl}&0\\ \hline 0&0&D1_{kl}\end{array}\right];$$

$$D1_{kl}=1/\omega\mu_0\cdot\left[k_l\sin\{(l+y_{1k}/a)1\pi/2\}\cos\Phi_{1k}\right.$$
$$\left.-jl/2a\cdot\cos\{(1+y_{1k}/a)l\pi/2\}\sin\Phi_{1k}\right]\exp(-jk_l x_{1k}),$$

$$E1=\begin{bmatrix}E1_{kn}^1\\ \hline E1_{kn}^2\\ \hline E1_{kn}^3\end{bmatrix};$$

$$E1_{kn}^i=jY_aJ_n'(2ak_a/\sqrt{3})\exp(-jn\Phi_k^i),$$

$$F1=\begin{bmatrix}F1_{kn}^1\\ \hline F1_{kn}^2\\ \hline F1_{kn}^3\end{bmatrix};$$

$$F1_{kn}^i=jY_aY_n'(2ak_a/\sqrt{3})\exp(-jn\Phi_k^i),$$

$$P=\begin{bmatrix}P_k^1\\ \hline P_k^2\\ \hline P_k^3\end{bmatrix};$$

$$P_k^1=-\sin\{(1+y_{1k}/a)\pi/2\}\exp(-jk_1x_{1k}),$$

$$P_k^2=P_k^3=0,$$

$$P1=\begin{bmatrix}P1_k^1\\ \hline P1_k^2\\ \hline P1_k^3\end{bmatrix};$$

$$P1_k^1=1/\omega\mu_0\cdot\left[k_1\sin\{(1+y_{1k}/a)\pi/2\}\cdot\cos\Phi_{1k}\right.$$
$$\left.+j\pi/2a\cdot\cos\{(1+y_{1k}/a)\pi/2\}\cdot\sin\Phi_{1k}\right]$$
$$\cdot\exp(-jk_1x_{1k}),$$

$$P1_k^2=P1_k^3=0,$$

$i=1,2,$ and 3
$k=1,2,\cdots,q_w$
$l=1,2,\cdots,m_w$
$n=-n_a,-n_a+1,\cdots,n_a.$

Equations (27) and (28) with (14) can be combined as

$$\left[\begin{array}{c|c}D&E+FZ\\ \hline D1&E1+F1Z\end{array}\right]\begin{bmatrix}d\\ b\end{bmatrix}=\begin{bmatrix}P\\ \hline P1\end{bmatrix}. \tag{29}$$

Equation (29) is in a form convenient for computing, in that the matrix Z is a function only of the ferrite properties, geometry, and location in the Y junction, while D, E, F, $D1$, $E1$, $F1$, P, and $P1$ are functions only of the waveguide geometry.

For the empty waveguide Y junction, the matrix Z is zero and the solution will give the scattering matrix of an empty Y junction. The truncation of the infinite series in the simultaneous equations (24) and (25) amounts to taking only a finite number of waveguide modes and cylindrical modes on the assumption that the neglected modes have much smaller amplitudes.

The conditions to indicate the accuracy of the results are as follows.

1) The rapidity of the convergence of the infinite series represents the fields. This can be indicated by observing the change in the mode amplitudes with the change of the number of matching points or with the change of the number of the waveguide and cylindrical modes. When the change in the mode amplitudes is insignificant, then the number of waveguide and cylindrical modes are considered to be sufficient.

2) The output power from the three-ports should equal the incident power

$$\sum_{i=1}^{M}|d_1^i|^2=1. \tag{30}$$

III. Testing of the Analysis

The empty and cylindrical ferrite post three-port junctions are taken to test the analysis.

A. Numerical Results of the Empty Three-Port Junction

The solution for the scattering matrix (29) for a Y junction with ferrite post has been derived. For the empty waveguide Y junction, the matrix Z is zero and the solution of (29) will give the scattering matrix of the empty Y junction. The cases of 3, 5, and 7 matching points on the boundary in each waveguide are considered. Accordingly, 3, 5, and 7 waveguide modes, and 5, 8, and 11 cylindrical modes are retained, respectively. In all three cases, the power condition (30) is satisfied to an accuracy of $\pm 10^{-8}$. However, the lowest order waveguide and cylindrical modes varied considerably when taking 3 and 5 points, while the difference between these modes in the cases of 5 and 7 points is small (0.03 dB).

The arguments of the scattering matrix eigenvalues are [5]

$$\theta_0=s_{11}+s_{12}+s_{13}$$
$$\theta_1=s_{11}+s_{12}\exp(j120^0)+s_{13}\exp(-j120^0)$$
$$\theta_{-1}=s_{11}+s_{12}\exp(-j120^0)+s_{13}\exp(j120^0) \tag{31}$$

where

$$s_{11}=d_1^1,\quad s_{12}=d_1^2,\quad\text{and}\quad s_{13}=d_1^3.$$

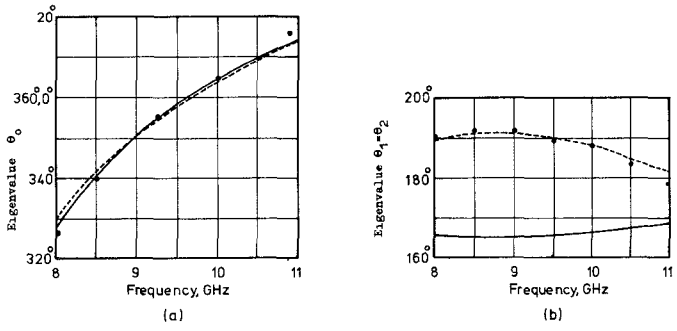

Fig. 3. Arguments of the scattering matrix eigenvalues for the empty 3-port junction:------values computed from this theory, ——— measured values given by [8], and ····· computed values given by [8].

The numerical results are shown in Fig. 3. The experimental results of Davies [8] and their theoretical calculations based on his analysis are also indicated in the same figure. The numerical results, based on the technique adopted in this paper, are found to be in excellent agreement with the previously published experimental results of Davies [8].

B. Numerical Results of Three-Port Junction with Central Cylindrical Ferrite Post

The matrix Z is constructed for the case of a cylindrical ferrite post (TT1-109) of radius 0.35 cm, and the numerical results of (29) are obtained. The cases of 3, 5, 7, and 9 matching points on the boundary in each waveguide are considered. It has been found that the values of the scattering matrix elements are dependent on the number of the waveguide modes and the corresponding cylindrical modes considered on the boundary between the waveguides and the air region (Fig. 4). They are independent of the number of the cylindrical modes considered on the ferrite–air interface; that is due to the fact that the individual modes are exactly matched along the ferrite–air interface for cylindrical ferrite posts, which is not the case for triangular ferrite post as will be seen later.

The convergence behavior of the scattering matrix elements is shown in Fig. 4. We see from Fig. 4 that 7 waveguide modes and 11 cylindrical modes are considered to be sufficient. The numerical values of the scattering matrix elements are obtained over the waveguide frequency range and are indicated in Fig. 5. The experimental results of Castillo and Davis [1] and their theoretical calculations based on the analysis of Davies are also indicated in the same figure. The numerical results are found to be in excellent agreement with the previously published experimental results of Castillo *et al.* [1].

C. Y Junction with a Triangular Ferrite Post

The construction of the matrices A, B, C, $A1$, $B1$, and $C1$ of (15) is required in order to have the matrix Z. The elements of these matrices are dependent on the matching points m along the ferrite–air interface (Fig. 6.).

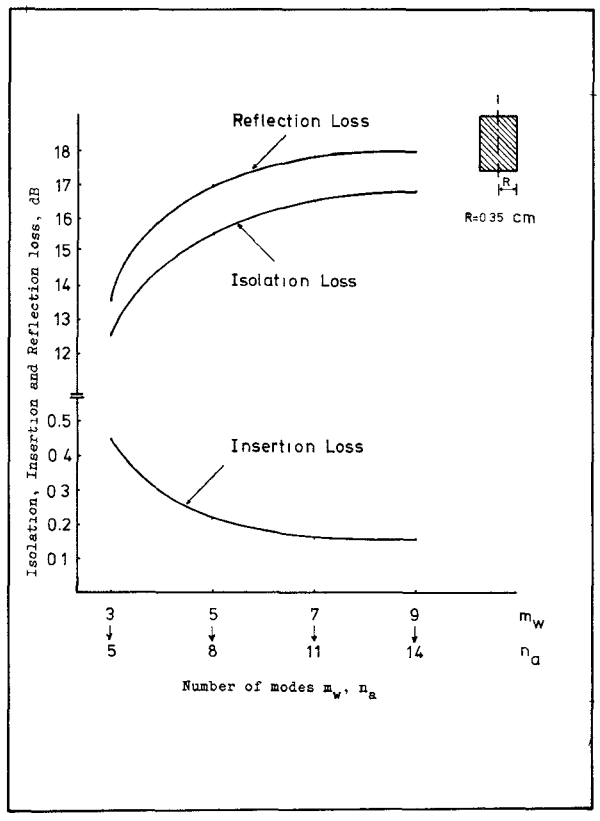

Fig. 4. Convergence behavior of the scattering matrix elements for a TT1-109 ferrite rod. m_w is the considered number of waveguide modes, and n_a is the corresponding number of cylindrical modes on the waveguide-air boundary ($f=10$ GHz).

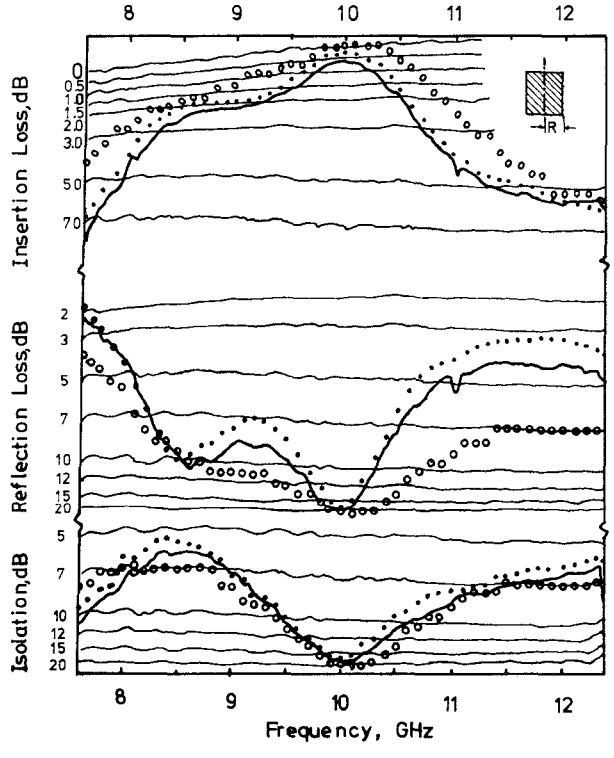

Fig. 5. Performance of a TT1-109 ferrite rod: ····· values computed from this theory, ——— measured values given by [1], and ○○○○○○○ computed values given by [1].

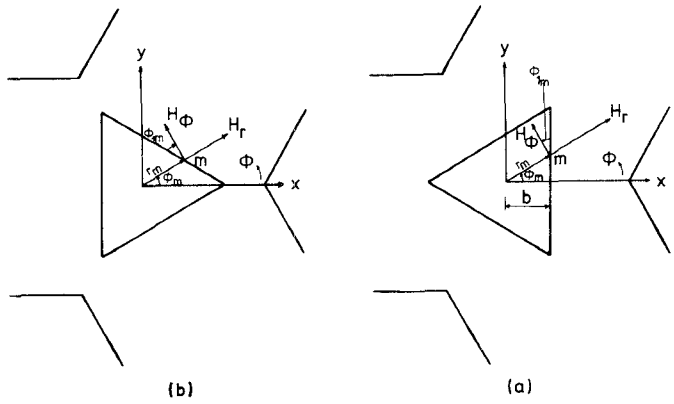

Fig. 6. Y junction with a triangular ferrite post.

For a matching point m at the ferrite side results in case of:

1) Points of the triangles are in the centers of the waveguides (Fig. 6(a))

$$r_m = b/\cos\Phi_{1m}$$
$$\Phi_m^i = \Phi_{1m} + (i-1)2\pi/3, \qquad -\pi/3 \leqslant \Phi_{1m} \leqslant \pi/3.$$

2) Sides of the triangles are in the centers of the waveguides (Fig. 6(b))

$$r_m = b/\cos\Phi_{1m}$$
$$\Phi_m^i = \Phi_{1m} + (i-1)2\pi/3 + \pi/3,$$
$$-\pi/3 \leqslant \Phi_{1m} \leqslant \pi/3 \text{ and } i = 1,2, \text{ and } 3.$$

D. Numerical Results of Triangular Post Y-Junction Circulator

The cases of 9, 11, 13, and 15 matching points on each side of the triangular ferrite are considered. Accordingly, 14, 17, 20, and 23 cylindrical modes at the ferrite–air interface are retained, respectively. In each case, 3, 5, 7, and 9 matching points in the boundary in each waveguide are considered. Accordingly, 3, 5, 7, and 9 waveguide modes and 5, 8, 11, and 14 cylindrical modes at the waveguide–air boundary are retained, respectively.

In all cases the power condition (30) is satisfied to an accuracy of $\pm 10^{-7}$. The convergence behavior of the scattering matrix elements is shown in Fig. 7. It should be noted that the values of the scattering matrix elements are heavily dependent on the number of the cylindrical modes considered for matching the fields on the ferrite–air interface. It is clear from Fig. 7 that 20 cylindrical modes for matching the fields at the ferrite–air interface, 7 waveguide modes, and 11 cylindrical modes for matching the fields on the waveguide–air boundary are considered to be sufficient, and are taken in the following numerical results. The numerical solution of the triangular ferrite post circulator is divided into two parts. The first considers the circulator characteristics, i.e., the scattering matrix, while

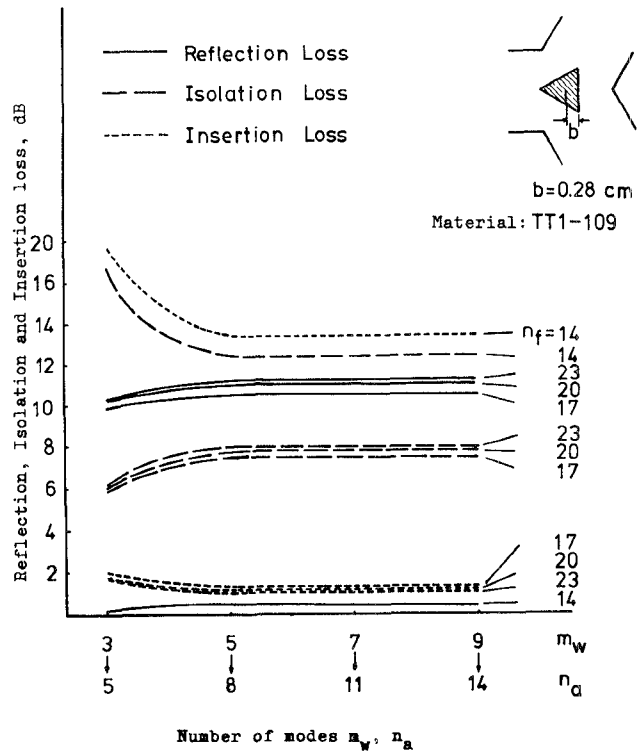

Fig. 7. Convergence behavior of the scattering matrix elements for a TT1-109 triangular ferrite post. m_w is the considered number of waveguide modes, n_a is the corresponding number of cylindrical modes on the waveguide-air boundary, and n_f is the considered number of cylindrical modes on the ferrite–air interface (f=9 GHz).

the second considers the field distribution inside the junction.

1) Circulator Characteristics: Numerical results are obtained for a TT1-109 ferrite sample. The internal dc magnetic field is $200/(4\pi 10^{-3})$ A/m. Fig. 8(a) shows the numerical results for the first arrangement, i.e., the points of the triangles are in the centers of the waveguides, and Fig. 8(b) shows the numerical results of the scattering matrix for the second arrangement. The frequency of the best isolation for the two arrangements is the same ($\sim$10 GHz). Their values for maximum isolation are -25 dB and -17 dB, respectively. It is to be noted that the performances obtained with the first arrangement are superior to those obtained with the second arrangement for the same dc magnetic field.

Comparing these results with the corresponding results of the cylindrical ferrite post circulator which have the same circulation direction at the same circulation frequency (Fig. 8(a)), it is clear that the performances obtained with the triangular ferrite post are better than those obtained with the cylindrical ferrite post.

2) Field Distributions: Once the constants a_n, b_n, and c_n are known, the electromagnetic field components at any point (r,Φ) within the junction are determined. Figs. 9(a) and (b) show the electric field and the tangential magnetic field component at the ferrite–air interface, respectively. The numerical values for both fields are obtained, as well

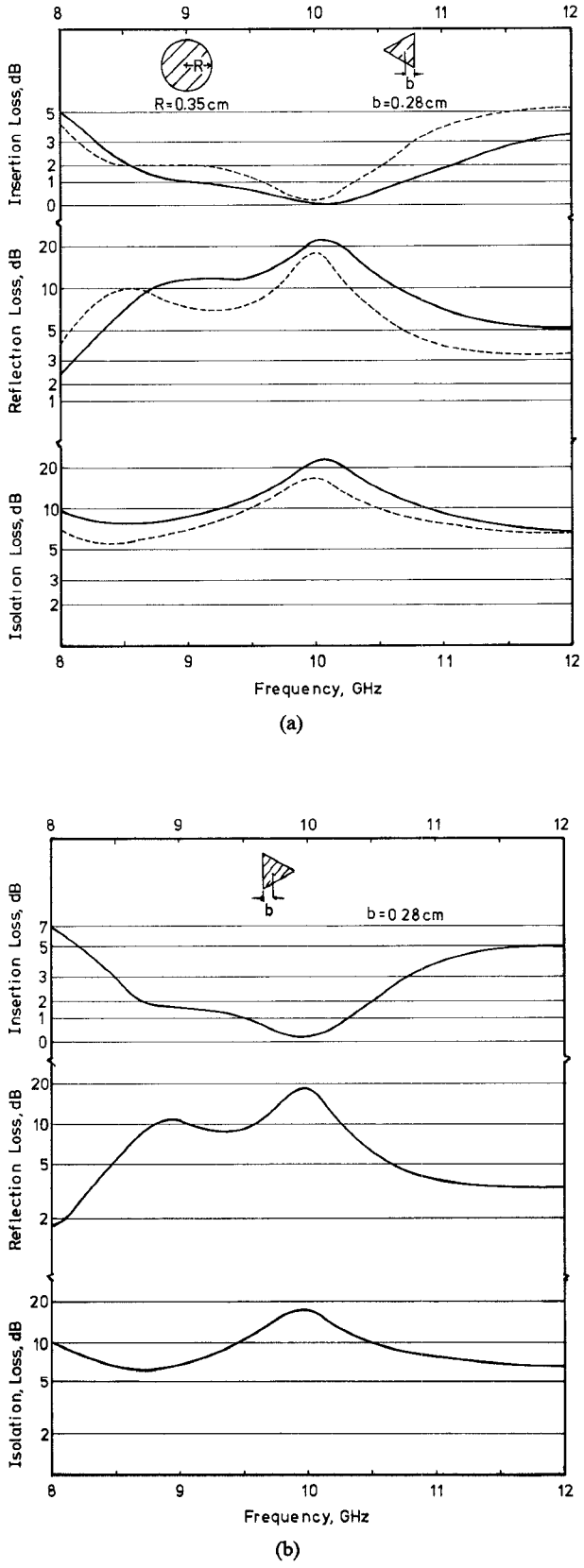

Fig. 8(a). ——— Performance of a TT1-109 triangular ferrite post for arrangement (a), and ------ performance of TT1-109 cylindrical ferrite rod. (b) Performance of a TT1-109 triangular ferrite post for the arrangement (b).

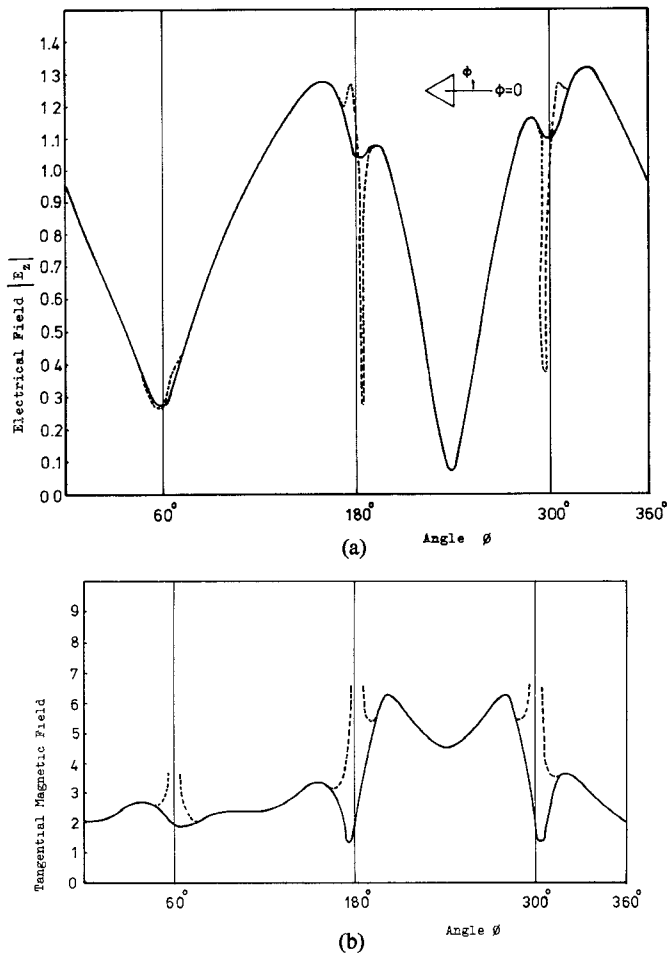

Fig. 9(a). The electric field distribution along the ferrite–air interface: ------ evaluated from the solution of the wave equation in the ferrite, and ——— evaluated from the solution of the wave equation in the air surrounding the ferrite on the ferrite–air interface. (b) The magnetic field distribution along the ferrite-air interface: ------ evaluated from the solution of the wave equation in the ferrite, and ——— evaluated from the solution of the wave equation in the air surrounding the ferrite on the ferrite–air interface.

from the solution of the wave equation in the ferrite post as from the solution in the surrounding air at the ferrite-air interface. The figures indicate that the electric field and the tangential magnetic field component are matched perfectly at the sides of the triangular ferrite. However, at the points of the triangular ferrite they are quite different. Increasing the number of matching points, i.e., the number of the cylindrical modes at the ferrite–air interface, in fact, corrects this situation. Nevertheless, it is not possible to match the fields at the edges exactly using the point-matching method.

Fig. 10 shows the electric field distribution in the Y junction with triangular ferrite post in the first arrangement (Fig. 8(a)) using a sample TT1-109 at the circulation frequency (10 GHz). This figure indicates that the electric field almost attains a minimum value at the isolated waveguide axis. At the axis of the input and the output ports, the electric fields are approximately equal although their phases are different.

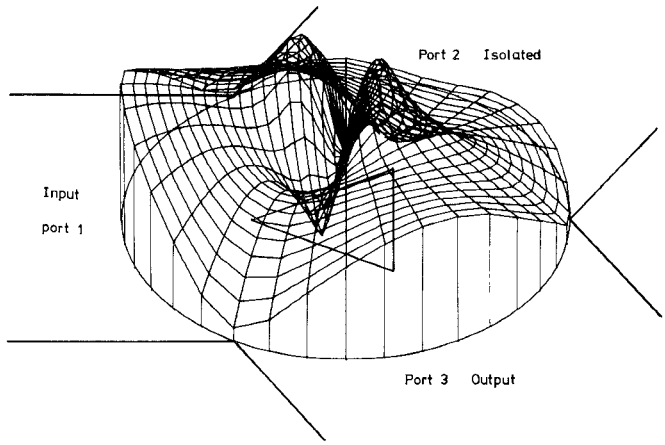

Fig. 10. The electric-field distribution inside the Y junction with a TT1-109 triangular ferrite post.

IV. Conclusion

The analysis given can be applied to the M-port waveguide junction when empty, or with general geometrical post of ferrite, dielectric, or conducting material. Comparison of theory with previously published experimental results on reciprocal three-port junctions and nonreciprocal three-port junctions with cylindrical ferrite posts gives excellent agreement. The agreement includes the eigenvalue arguments of the nondegenerate or degenerate eigenvalues for reciprocal three-port junctions and the frequency of best isolation, the value of isolation at this frequency, and also the general shape of the reflection-coefficient characteristics for nonreciprocal three-port junctions with cylindrical ferrite post.

To demonstrate the value of the adopted technique for a junction with a general geometrical full-height post, the triangular ferrite post in a Y junction is taken as an example. Two arrangements of the triangular ferrite post in the junction are studied. The first arrangement, in which the points of the triangles are in the centers of the waveguides, gives better characteristics: namely, higher isolation and reflection loss, and smaller insertion loss at the circulation frequency than that from the second arrangement in which the sides of the triangles are in the centers of the waveguides. Moreover, the obtained characteristics for the Y junction with a triangular ferrite post are better than the characteristics in the case of a cylindrical ferrite post for the same circulation frequency.

The power of this technique is further strengthened by the fact that it reveals information from which the electromagnetic field components inside the junction are obtained. Furthermore, it can be used to study the effect of the ferrite geometry on the circulator performance; it means that it is possible to optimize the form of the cross section of the ferrite to find the best possible circulator structure.

References

[1] J. B. Castillo and L. E. Davis, "Computer-aided design of three-port waveguide junction circulators," *IEEE Trans. Microwave Theory Tech.*, vol. MTT-18, pp. 25–34, Jan. 1970.

[2] ——, "A higher order approximation for waveguide circulators," *IEEE Trans. Microwave Theory Tech.* (short paper), vol. MTT-20, pp. 410–412, June 1972.

[3] M. E. El-Shandwily, A. A. Kamal, and E. A. F. Abdallah, "General field theory treatment of H-plane waveguide junction circulators," *IEEE Trans. Microwave Theory Tech.*, vol. MTT-21, pp. 392–403, June 1973.

[4] J. Helszajn and F. C. Tan, "Design data for radial-waveguide circulators using partial-height ferrite resonators," *IEEE Trans. Microwave Theory Tech.*, vol. MTT-23, pp. 288–298, Mar. 1975.

[5] B. Owen, "The identification of modal resonances in ferrite loaded waveguide Y-junctions and their adjustment for circulation," *Bell Syst. Tech. J.*, vol. 51, pp. 595–627, Mar. 1972.

[6] Y. Akaiwa, "Operation modes of a waveguide Y circulator," *IEEE Trans. Microwave Theory Tech.* (short paper), vol. MTT-22, pp. 954–960, Nov. 1974.

[7] ——, "Mode classification of a triangular ferrite post for Y-circulator operation," *IEEE Trans. Microwave Theory Tech.* (short paper), vol. MTT-25, pp. 59–61, Jan. 1977.

[8] J. B. Davies, "An analysis of m-port symmetrical H-plane waveguide junction with central ferrite post," *IRE Trans. Microwave Theory Tech.*, vol. MTT-10, pp. 596–604, Nov. 1962.